Subcellular Interactions between Parallel Fibre and Climbing Fibre Signals in Purkinje Cells Predict Sensitivity of Classical Conditioning to Interstimulus Interval

JEANETTE HELLGREN KOTALESKI, DAVID LESTER, AND KIM T. BLACKWELL

George Mason University, School of Computational Sciences and The Krasnow Institute for Advanced Studies

Classical conditioning of the nictitating membrane response requires a specific temporal interval between conditioned stimulus and unconditioned stimulus, and produces an increase in Protein Kinase C (PKC) activation in Purkinje cells. To evaluate whether biochemical interactions within the Purkinje cell may explain the temporal sensitivity, a model of PKC activation by Ca^{2+}, diacylglycerol (DAG), and arachidonic acid (AA) is developed. Ca^{2+} elevation is due to CF stimulation and IP3 induced Ca^{2+} release (IICR). DAG and IP_3 result from PF stimulation, while AA results from phospholipase A2 (PLA_2). Simulations predict increased PKC activation when PF stimulation precedes CF stimulation by 0.1 to 3 s. The sensitivity of IICR to the temporal relation between PF and CF stimulation, together with the buffering system of Purkinje cells, significantly contribute to the temporal sensitivity.

Keywords—classical conditioning, Purkinje cell, Protein Kinase C, IP_3 induced calcium release, computer modeling, LTD

Introduction

IN CLASSICAL CONDITIONING, memory storage depends critically on the order as well as the timing of the conditioned and unconditioned stimuli. Classical conditioning of the rabbit nictitating membrane response is performed using a tone as the conditioned stimulus (CS) and an air puff to the eye as the unconditioned stimulus (US). Conditioning occurs only if the CS is given between 80 and 3000 ms prior to the US (Gormezano, Kehoe & Marshall, 1983).

The cerebellum is crucial for memory storage in both delay and trace conditioning (Green & Woodruff-Pak, 2000; Gruart, Guillazo-Blanch, Fernandez-Mas, Jimenez-Diaz & Delgado-Garcia, 2000; Ivkovich, Paczkowski & Stanton, 2000; McCormick & Thompson, 1984; Ryou, Cho Kim, 2001; Thompson, 1986; Thompson & Kim, 1996; Stanton, 2000;

Address for Correspondence: Jeanette Hellgren Kotaleski, Dept. of Numerical Analysis and Computing Science, Royal Institute of Technology, S-100 44 Stockholm, Sweden Fax: +46-8-7900930, Phone: +46-8-7906903, E-mail: jeanette@nada.kth.se

Integrative Physiological & Behavioral Science, October–December 2002, Vol. 37, No. 4, 265–292.

Woodruff-Pak, Lavond & Thompson, 1985). Information about the CS (tone) is conveyed by parallel fibres (PFs) while climbing fibers (CFs) carry the US (Steinmetz, 2000; Thompson, 1986; Thompson & Krupa, 1994). Both PFs and CFs synapse on Purkinje cells, the former on the dendritic spines activating AMPA and metabotropic glutamate receptors (mGluR), while CFs activate AMPA receptors leading to generation of Ca^{2+} spikes and influx of Ca^{2+}. *In vivo,* learning-related changes in neuronal firing are seen in both the cerebellar cortex (lobule HVI) and in the deep nuclei (interpositus) (Gould & Steinmetz, 1996; Katz & Steinmetz, 1997). *In vitro* cellular correlates of classical conditioning found in Purkinje cells of lobule HVI include an increase in excitability (Schreurs, Tomsic, Gusev & Alkon, 1997), due to a reduction in transient potassium currents, and translocation of PKC from the cytosol to the membrane (Freeman Jr, Schaarenberg, Olds & Schreurs, 1998).

As part of identifying the PF and CF interactions leading to memory storage, Schreurs, Oh & Alkon (1996) and Schreurs, Tomsic, Gusev & Alkon (1997) have developed a PF and CF stimulation protocol that maintains an interstimulus interval (ISI) and intertrial interval (ITI) used for classical conditioning of rabbits. PF stimulation occurs at a frequency of 100 Hz for 80 ms (8 pulses), and CF stimulation occurs at a frequency of 20 Hz for 100 ms (3 pulses). When applied to a slice preparation the stimulation protocol causes pairing specific long-term depression, denoted PSD (Schreurs, Oh & Alkon, 1996), which is prevented by blocking PKC activation or Ca^{2+} elevation (Freeman Jr, Shi & Schreurs, 1998). Thus, both *in vivo* and *in vitro* data support that PKC activation is critical for classical conditioning by phosphorylating potassium channels, thereby contributing to an increase in excitability, and by phosphorylating AMPA receptors, thereby contributing to synaptic depression.

The mechanism underlying the temporal specificity of classical conditioning remains a mystery. Several proteins require paired stimuli for their activation, e.g., the NMDA receptor requires both depolarization and glutamate; PKC requires calcium, diacylglycerol, and arachidonic acid. However, temporal requirements similar to classical conditioning have not been demonstrated for these or any other molecule. Identifying the molecule(s), or parts of biochemical pathways, that require such temporal specificity for their activation is likely to shed light on the mechanism of associative memory storage.

Thus, the aim of the present study is to evaluate to what extent the activation requirements of PKC could underlie the temporal sensitivity of classical conditioning. We develop a model of the biochemical pathways activated by PF and CF stimulation, and perform simulations using stimulation protocols developed by Schreurs, Oh & Alkon (1996), as well as additional interstimulus intervals. The present results suggest that a persistently active form of PKC is formed in significantly larger amounts if the ISI between the PF and CF stimuli is similar to the CS-US intervals that produce classical conditioning (Gormezano, Kehoe & Marshall, 1983).

Methodology

The present model includes a minimal number of biochemical pathways activated by PF and CF stimulation during classical conditioning in order to minimize the number of parameters. Only signaling pathways commonly agreed on to be activated (Daniel, Levenes & Crepel, 1998) are taken into account. The model thus consists of three separate sets of biochemical reactions (see Fig. 1). One set of reactions describes DAG and IP_3 production and Ca^{2+} release in response to PF stimulation. Another set of reactions de-

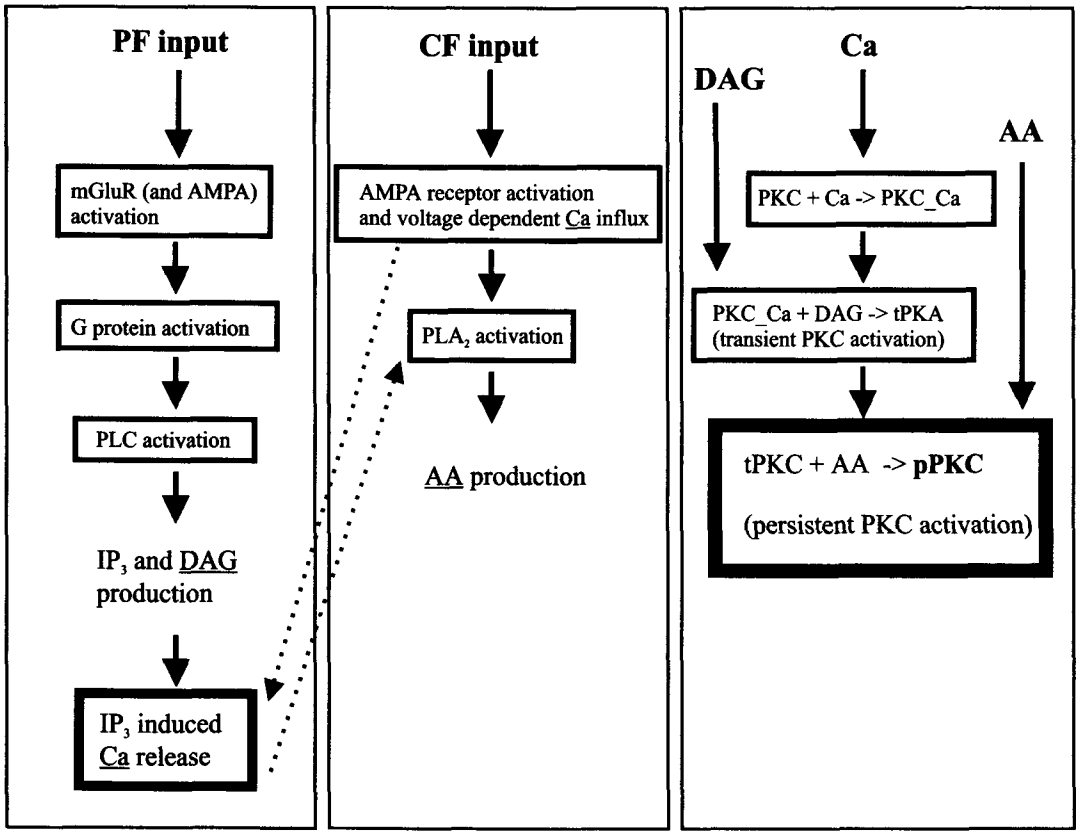

FIG. 1. Signaling pathways included in the model. The three separate sets of biochemical reactions are illustrated in three different columns. Heavy box lines indicate reactions whose products (underlined) are substrates for PKC. Dotted lines indicate a point of interaction between the PF and CF pathways. The output of the model, pPKC, is indicated in bold.

scribes AA production in response to Ca^{2+} elevation. The third set of biochemical reactions describes PKC activation in response to calcium, DAG, and AA elevation.

In this study the rate constants for the different biochemical reactions are, when possible, inferred from Purkinje cell data or else from neural tissue. Rate constants for PKC activation are adjusted independently of PF and CF stimuli using constant concentrations of calcium, DAG, and AA. The rate constants of the PF stimulation pathway are adjusted independently of the rate constants describing AA production. Rate constants relating to IP_3 production and calcium release are adjusted to match calcium imaging data from experiments on cerebellar Purkinje cells.

PF stimulation

PFs activate Purkinje cell mGluR receptors resulting in diacylglycerol (DAG) and inositol trisphosphate (IP_3) production via activation of G-proteins and phospholipase C (PLC) (Canepari, Papageorgiou, Corrie, Watkins & Ogden, 2001; Hirono, Konishi & Yoshioka, 1998; Hirono, Sugiyama, Kishimoto, Sakai, Miyazawa, et al., 2001; Netzeband, Parsons,

Sweeney & Gruol, 1997). When glutamate binds to the mGluR (type 1), the complex catalyzes binding of the α subunit of the G protein to GTP. The resulting active G protein (aG) then activates PLC (aPLC). The corresponding rate constants are obtained from Smrcka, Hepler, Brown & Sternweis (1991) and Mukhopadhyay & Ross (1999) and adjusted to reproduce an increase of aG with the number of PF stimuli as found by Tempia, Miniaci, Anchisi & Strata (1998).

Active PLC hydrolyzes PIP_2 to produce DAG and IP_3 (Smrcka, Hepler, Brown & Sternweis, 1991). The reaction kinetics are set to produce the concentration of IP_3 estimated in response to PF activation (Finch & Augustine, 1998; Takechi, Eilers & Konnerth, 1998) and are constrained by rate constants measured by Smrcka, Hepler, Brown & Sternweis (1991). The half life of IP_3 has been estimated (Allbritton, Meyer & Stryer, 1992; Finch & Augustine, 1998; Wang, Alousi & Thompson, 1995). DAG is de-activated by phosphorylation, but the rate of DAG de-activation in Purkinje cells is not known. In the model the DAG rate of de-activation (referred to as decay rate) is set to be slower than for IP3 and then varied to investigate whether the results are sensitive to DAG decay.

These biochemical steps are modeled according to the following scheme:

$$Glu + mGluR \underset{k1_b}{\overset{k1_f}{\rightleftharpoons}} Glu\_mGluR \tag{1}$$

$$Glu\_mGluR + G \underset{k2_b}{\overset{k2_f}{\rightleftharpoons}} G\_Glu\_mGluR \xrightarrow{k2_{cat}} aG + Glu\_mGluR \tag{2}$$

$$aG \xrightarrow{k3_f} G \tag{3}$$

$$aG + PLC \underset{k4_b}{\overset{k4_f}{\rightleftharpoons}} aPLC \tag{4}$$

$$aPLC + PIP_2 \underset{k5_b}{\overset{k5_f}{\rightleftharpoons}} aPLC\_PIP_2 \xrightarrow{k5_{cat}} aPLC + IP_3 + DAG \tag{5}$$

$$IP_3 \xrightarrow{k6_f} decayIP_3 \tag{6}$$

$$DAG \xrightarrow{k7_f} decayDAG \tag{7}$$

Both the rate-limiting inactivation of aG and regeneration of G protein from Gα-GDP and GBγ are implicit in eq. (3) that describes aG degradation (see also Destexhe, Mainen

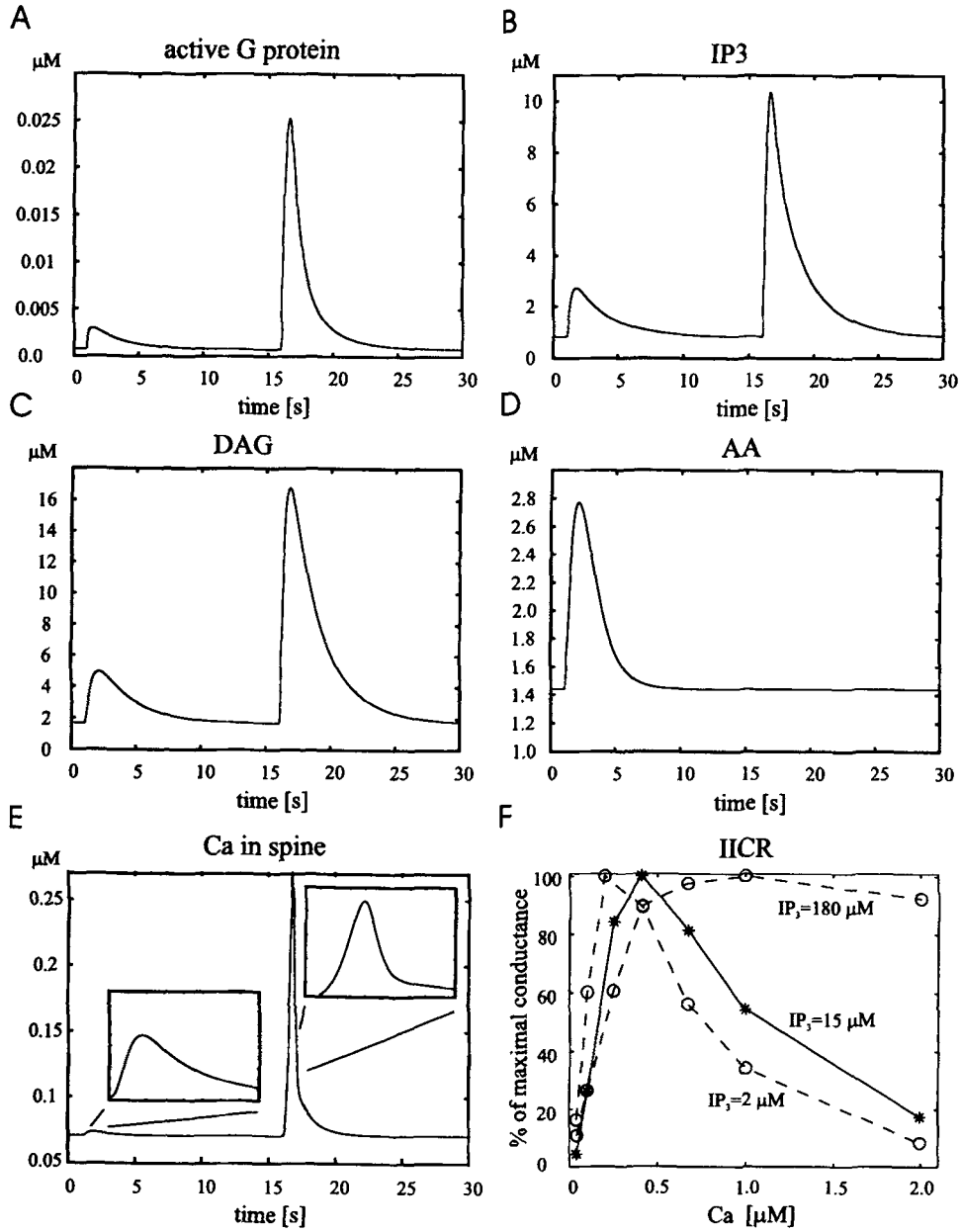

FIG. 2. The differences in the simulated G-protein activation (A), IP_3 (B) and DAG (C) following 1 PF pulse given at time 1 s, or 8 PF pulses given at time 16 s. In (D) the resulting AA response following 3 CF pulses given at time 1 s is illustrated. Here, the CF input is given at a resting level of DAG. If, however, the DAG level is increased when the CF input arrives higher AA peak levels are seen. A low background level of glutamate (0.1 μM) as well as Ca^{2+} (0.07 μM) is used in all simulations. (E) shows that the Ca^{2+} released due to the IP_3 resulting from 1 PF pulse (given at time 1 s) is hardly visible, while 8 PF pulses (given at time 16 s) increase Ca^{2+} significantly above the rest level. This is due to the requirement of approximately 10μM IP_3 to reach the threshold for significant amounts of IICR (Khodakhah & Ogden, 1995; Finch & Augustine, 1998; Takechi, Eilers & Konnerth, 1998). In (F) the bell-shaped dependence on Ca^{2+} for IP_3 = 15 μM is shown for our model (solid line). For comparison the Ca^{2+} dependence for lower and higher IP_3 values, as measured in isolated cerebellar microsomes, are also shown (dashed lines; data replotted from Kaftan, Ehrlich & Watras, 1997). Note that in cerebellar slices the lower IP_3 value of 2 μM would not cause significant Ca^{2+} release.

& Sejnowski, *1994).* The behavior of this set of reactions is illustrated in Figure 2. These graphs compare one PF pulse, delivered at 1 s, with eight PF pulses, delivered at *16 s.* Each PF pulse is assumed to result in 1 mM of glutamate for 1 ms. An increase in the number of pulses leads to a larger amount of aG (Fig. 2A), as demonstrated by Tempia, Miniaci, Anchisi & Strata *(1998).* This increase in aG with eight PF pulses results in a larger concentration of IP_3 (Fig. 2B) and DAG (Fig. 2C) following eight pulses as compared to one pulse. The DAG concentration is greater than the IP_3 due to the slower decay rate of the former. The concentration of IP_3 produced by eight PF pulses, approximately 10 μM, is comparable to that demonstrated by Finch & Augustine (1998).

AA production

An elevation in Ca^{2+} activates phospholipase A2 *(PLA_2),* which produces arachidonic acid (AA) from membrane phospholipids (PL), see, e.g., Stella, Pellerin & Magistretti (1995) and references therein. This was included in the model based on experiments by Linden (1995) showing that Purkinje cell LTD, which also depends on PKC, requires PLA_2 activation, see also Reynolds & Hartell (2001).

$$PLA_2 + Ca \underset{k8_b}{\overset{k8_f}{\rightleftharpoons}} aPLA_2 \tag{8}$$

where $k8_f = DAG \bullet k8_0$

$$aPLA_2 + PL \underset{k9_b}{\overset{k9_f}{\rightleftharpoons}} PLA_2\_PL \xrightarrow{k9_{cat}} aPLA_2 + AA \tag{9}$$

$$AA \xrightarrow{k10_f} decayAA \tag{10}$$

The forward rate constant of eq. *(8)* is furthermore modeled as being proportional to the DAG concentration. This allows DAG to produce a facilitatory effect on PLA_2 activity (Leslie & Channon, 1990), either directly, or by increasing the availability of the substrate, similar to the effect of mild detergents on PLA_2 activity observed in biochemical assays (Petit, De Block & De Potter, 1995). The decay of AA is due to re-incorporation into phospholipids. Rate constants for these reactions are obtained from Petit, De Block & De Potter (1995); Stella, Pellerin & Magistretti (1995); and Pete & Exton (1996). Figure 2D shows the AA signal following 3 CF pulses delivered at 1 s.

PKC activation

PKC binds Ca^{2+} and this complex (PKC_Ca) together with DAG form a transiently active form, tPKC. When AA is added, a more persistent form of PKC, pPKC, results. The form of these reactions and their kinetics are derived from Bramham, Alkon & Lester (1994); Lester & Bramham (1993); Oancea & Meyer (1998); Schacter, Lester & Alkon (1996); Shinomura, Asaoka, Oka, Yoshida & Nishizuka (1991); Shirai, Kashiwagi, Yagi, Sakai & Saito (1998); and Shirai, Sakai & Satir (1998), see eq. (11–13). Rate constants are adjusted to replicate the experiments by Oancea & Meyer (1998) and Shirai, Sakai & Satir

(1998) that evaluate PKC translocation in response to DAG, AA and Ca^{2+}, *as* described in Yang, Hellgren Kotaleski & Blackwell (2000).

$$PKC + Ca \underset{k11_b}{\overset{k11_f}{\rightleftarrows}} PKC\_Ca \tag{11}$$

$$PKC\_Ca + DAG \underset{k12_b}{\overset{k12_f}{\rightleftarrows}} tPKC \tag{12}$$

$$tPKC + AA \underset{k13_b}{\overset{k13_f}{\rightleftarrows}} pPKC \tag{13}$$

All of the biochemical reaction steps listed above can be generalized to the following form:

$$\sum_{i=1}^{n} [Substrate_i] \underset{k_b}{\overset{k_f}{\rightleftarrows}} \sum_{i=1}^{n} [Product_i] \tag{14}$$

Then, given an initial amount of each reactant, the amount of $Substrate_i$ can be calculated as:

$$\frac{d[Substrate_i]}{dt} = k_b \prod_{i=1}^{n} [Product_i] - k_f \prod_{i=1}^{n} [Substrate_i] \tag{15}$$

Sources of Ca^{2+}

There are two sources of Ca^{2+} in the model. One results from CF activation of voltage dependent Ca^{2+} channels. The effect of CF activation is modeled as a transient increase in the calcium concentration in the dendritic shaft (Miyakawa, Lev-Ram, Lasser-Ross & Ross, 1992; De Schutter & Bower, 1994). The Ca^{2+} pulse in the shaft is given a peak value of 1 μM, which is within the range of estimated Ca^{2+} elevations during complex spiking (e.g Kano, Garaschuk, Verkhratsky & Konnerth, 1995; Maeda, Ellis-Davies, Ito, Miyashita & Kasai, 1999). The Ca^{2+} in the shaft decays with a half time of less than 50 ms (Miyakawa, Lev-Ram, Lasser-Ross & Ross, 1992) and diffuses from the shaft into the spines (see Callaway, Lasser-Ross & Ross, 1995). The expression for the apparent diffusion coefficient ($Dapp = (Dca + k_H(Ca)Dh)/(1 + k_L + k_H(Ca))$ and the associated parameters are as in Maeda, Ellis-Davies, Ito, Miyashita & Kasai (1999). The spine neck is represented by a cylinder of diameter 0.2 μm and length of 0.66 μm, and the spine head is represented by a sphere with a diameter 0.54 μm (De Schutter & Bower, 1994). The 1 μM elevation in shaft Ca^{2+} produces a 0.4 μM elevation in spine Ca^{2+} with a delay in the peak of 80 ms. There is some evidence of voltage dependent channels in the spine head (Sabatini, Maravall & Svoboda, 2001) which would be activated by CF stimulation. Including voltage dependent channels in the spine head would slightly decrease the delay between CF stimulation and Ca^{2+} elevation.

The second source of Ca^{2+} is due to IP_3 induced Ca^{2+} release (IICR) from the endoplasmic reticulum (ER). This is included in the model because recent Ca^{2+} imaging results using short trains of PF stimulation have shown that Ca^{2+} release occurs in response to a PF stimulation pattern that is physiologically realistic (Finch & Augustine, 1998; Miyata, Finch, Khiroug, Hashimoto, Hayasaka, et al., 2000; Takechi, Eilers & Konnerth, 1998; Wang, Denk & Hausser, 2000). Therefore the possible role of Ca^{2+} release in classical conditioning is evaluated, although this has not been a necessary requirement in all preparations studying LTD (Daniel, Levenes & Crepel, 1998; Hemart, Daniel, Jaillard & Crepel, 1995). We use a Hodgkin-Huxley like formalism to describe IP_3 induced Ca^{2+} release (Li & Rinzel, 1994). The activation depends on both IP_3 and Ca , while the inactivation depends only on Ca^{2+}. Ca^{2+} in the spine is calculated as in Li & Rinzel (1994) (see also Jafri & Keizer, 1997):

$$\frac{dCa\_spine}{dt} = \begin{cases} \beta \cdot \Big(c1 \cdot \big(r1 \cdot m_o^3 h^3 + r2 \big) \cdot \big(Ca\_ER - Ca\_spine \big) - \\ r3 \cdot \big(Ca\_spine \big)^2 \,/\, \big(K3^2 + (Ca\_spine)^2 \big) \Big) + \text{diffusion} \end{cases} \tag{16}$$

where:

$$\begin{cases} m_o = (IP_3 \,/\, (IP_3 + d1)) \cdot (Ca\_spine \,/\, (Ca\_spine + d5)) \\ Q2 = d2(IP_3 + d1) \,/\, (IP_3 + d3) \\ h_o = Q2 \,/\, (Q2 + Ca\_spine) \\ \tau_h = 1 \,/\, (a2(Q2 + Ca\_spine)) \\ dh \,/\, dt = (h_o - h) \,/\, \tau_h \end{cases} \tag{17}$$

Diffusion of Ca^{2+} along the length of the spine is calculated numerically as:

$$\frac{dCa(x)}{dt} = \frac{Dapp(x) \cdot ([Ca(x+dx) - Ca(x)] + [Ca(x-dx) - Ca(x)]) \cdot Area(x)}{dx \cdot Volume(x)} \tag{18}$$

Purkinje cell data are used to adjust the parameters (Finch & Augustine, *1998;* Khodakhah & Ogden, 1995). $a2$ is set to 8 $\mu M^{-1}s^{-1}$ to yield a τ_h of *25* ms at an IP_3 = 20 μM as shown experimentally, see Khodakhah & Ogden (1995). Setting parameters $d1$ and $d3$ to 10 μM, and $d2$ and $d5$ to 0.4 μM produces an apparent threshold value for IP_3 of 10 PM (Khodakhah & Ogden, 1995) (compare Fig. 2B with Fig. 2E). This concentration of IP_3 needed to activate IP_3 gated Ca^{2+} channels in Purkinje cells is higher than that needed for purified cerebellar microsomes (Watras, Bezprozvanny & Ehrlich, *1991).* This may be due to the presence of an inhibitor of the IP_3 receptor (Watras, Orlando & Moraru, 2000). With these parameters, the steady state conductance of the IP_3 exhibits a bell-shaped dependence on Ca^{2+} concentration, with a maximum when Ca^{2+} = 0.4 μM (Kaftan, Ehrlich & Watras, 1997) (see Fig. 2F). The maximal conductance of the channel, $r1$, is 23250 s^{-1}; passive leakage of calcium from the ER (Ca_{ER} = 500 μM) to the cytosol, $r2$, is 0.28 s^{-1}; r3, which represents maximal pump capacity is *500* μMs^{-1}; c1, the ratio of ER to cytosol volume, is 0.185; and the pump affinity, $K3$, is 0.3 μM. This simplified IICR model reproduces the fast activation and slow inactivation of IICR by Ca^{2+} and can account for IP_3 uncaging experimental data for the range of IP_3 concentrations that are used in the

TABLE 1
Parameters used in eq. 1–14

description	*parameters*	*values*
rate constants, eq.1–7	$k1_f$	1 $\mu M^{-1}s^{-1}$
	$k1_b$	5000 s^{-1}
	$k2_f$	15 $\mu M^{-1}s^{-1}$
	$k2_b$	7.2 s^{-1}
	$k2_{cat}$	1.8 s^{-1}
	$k3_f$	10 s^{-1}
	$k4_f$	100 $\mu M^{-1}s^{-1}$
	$k4_b$	100 s^{-1}
	$k5_f$	192 $\mu M^{-1}s^{-1}$
	$k5_b$	768 s^{-1}
	$k5_{cat}$	192 s^{-1}
	$k6_f$	4 s^{-1}
	$k7_f$	2 s^{-1}
rate constants, eq 8–13	$k8_0$	0.3 $\mu M^{-1}s^{-1}$
	$k8_b$	3 s^{-1}
	$k9_f$	22 $\mu M^{-1}s^{-1}$
	$k9_b$	444 s^{-1}
	$k9_{cat}$	111 s^{-1}
	$k10_f$	1 s^{-1}
	$k11_f$	20 $\mu M^{-1}s^{-1}$
	$k11_b$	50 s^{-1}
	$k12_f$	0.015 $\mu M^{-1}s^{-1}$
	$k12_b$	0.15 s^{-1}
	$k13_f$	0.001 $\mu M^{-1}s^{-1}$
	$k13_b$	0.02 s^{-1}
initial values, etc	glutamate pulse	1000 μM duration 1ms
	background glutamate	0. 1 μM
	resting Ca^{2+} conc	0.07 μM
	mGluR	5 μM
	G protein	25 μM
	PLC	5 μM
	PIP_2	25 μM
	PLA_2	1 μM
	PL	30 μM
	PKC	10 μM

present model. The fraction of free Ca^{2+} due to Ca^{2+} buffers is represented by the parameter β in eq. (16). The formulas and parameters for calculating β ($\beta = 1/(1 + k_L + k_H(Ca^{2+})$; where k_H and k_L refers to binding ratio of a high and low affinity buffer, respectively) is as in Maeda, Ellis-Davies, Ito, Miyashita & Kasai (1999), where also a thorough evaluation and motivation of this modeling approach is provided. In summary, this steady state approximation to the effect of buffers is valid because the buffer reactions proceed very quickly compared to diffusion and IICR. The calcium flux due to diffusion is either into or out of the spine, depending on the concentration gradient.

Simulations

To evaluate the role of various second messengers and interactions, simulations were performed with models in which the role of certain "components" were evaluated by

TABLE 2
Abbreviations

Abbreviation	*Full name*
AA	arachidonic acid
CF(s)	climbing fibre(s)
CR	conditioned response
CS	conditioned stimuli
DAG	diacylglycerol
G/aG	G protein / active form of G protein
IICR	IP_3 induced Ca^{2+} release
IP_3	inositol trisphosphate
ISI	interstimulus interval
LTD/PSD	long term depression / pairing specific long term depression
mGluR	metabotropic glutamate receptor
PF(s)	parallel fibre(s)
PIP_2	phosphatidylinositol-bisphosphate
PL	phospholipid
PLC	phospholipase C
PKC	protein kinase C
pPKC	persistently active form of PKC
tPKC	transiently active form of PKC

removing them. (1) In one reduced model, the sole source of calcium was diffusion from the dendritic shaft. Release of calcium from intracellular stores was not included in this model. (2) In another model, the fraction of free Ca^{2+} was set to be constant (β above was set to be constant) meaning that the buffers that regulate free Ca^{2+} are nonsaturating.

The differential equations describing the biochemical reactions were implemented in XPP (http://www.math.pitt.edu/~bard/xpp/xpp.html). The activation patterns of parallel and climbing fibres were the same as that used by Schreurs, Oh & Alkon (1996). 8 PF pulses, 100 Hz, were combined with 3 CF pulses, 20 Hz, and this was repeated every 30s. Different intervals between the onset of PF and CF stimulation were tested as indicated below. We also compared results using longer PF trains (Schreurs & Alkon, 1993) as well as a conventional LTD stimulation protocol (Karachot, Kado & Ito, 1994).

Results

Ca^{2+} *dynamics*

The amount of calcium released in response to PF stimulation depends on the number of PF pulses as shown in Figure 2 and is in addition sensitive to the ISI between PF and CF. This latter behavior is an emergent property of the model. Figure 3A shows the Ca^{2+} concentration in the spine in response to 8 PF pulses given both at times 1 s and 16 s; three CF pulses are given 250 ms after the onset of PF stimulation at time 1 s, while they are given 250 ms before the PF input at time 16 s. An amplification in the calcium released is seen when Ca^{2+} is transiently increased in the dendritic shaft during the early phase of IP_3 elevation. If instead the Ca^{2+} elevation occurs before, or simultaneously with, the 8 PF pulses, the IICR response is reduced, and the Ca^{2+} response seen in the spine is mostly due

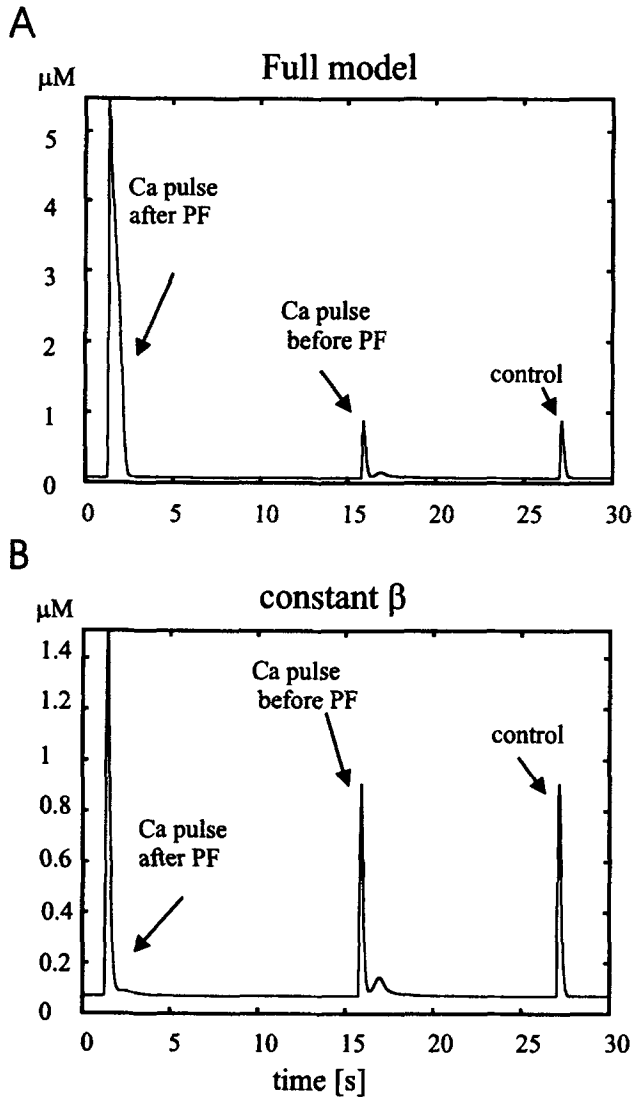

FIG. 3. Effect of PF and CF stimulation on spine Ca^{2+}. In (A) Ca^{2+} signals in the spine are shown when a transient Ca^{2+} elevation (3 CF pulses, 20 Hz) is given before or after an 8 PF train (100 Hz). Only the CF input is given at time 27s for comparison. 8 PF are given at times 1 and 16 s and combined with the CF input given either 250 ms before or 250 ms after the onset of the PF stimulation. In (B), ß is kept constant at 0.0008 implying that the Ca^{2+} buffers are nonsaturating.

to diffusion of Ca^{2+} from the shaft (compare with response of CF stimuli alone at 27 s in Fig. 3A).

Figure 3B illustrates the significant role of Ca^{2+} buffers by repeating the simulations in Figure 3A using the model with non-saturating buffers. The facilitatory effect on IICR when increasing Ca^{2+} transiently after the PF input is much less apparent although still a supralinear Ca^{2+} summation occurs.

The mechanism underlying the facilitatory or inhibitory response of a transient Ca^{2+}

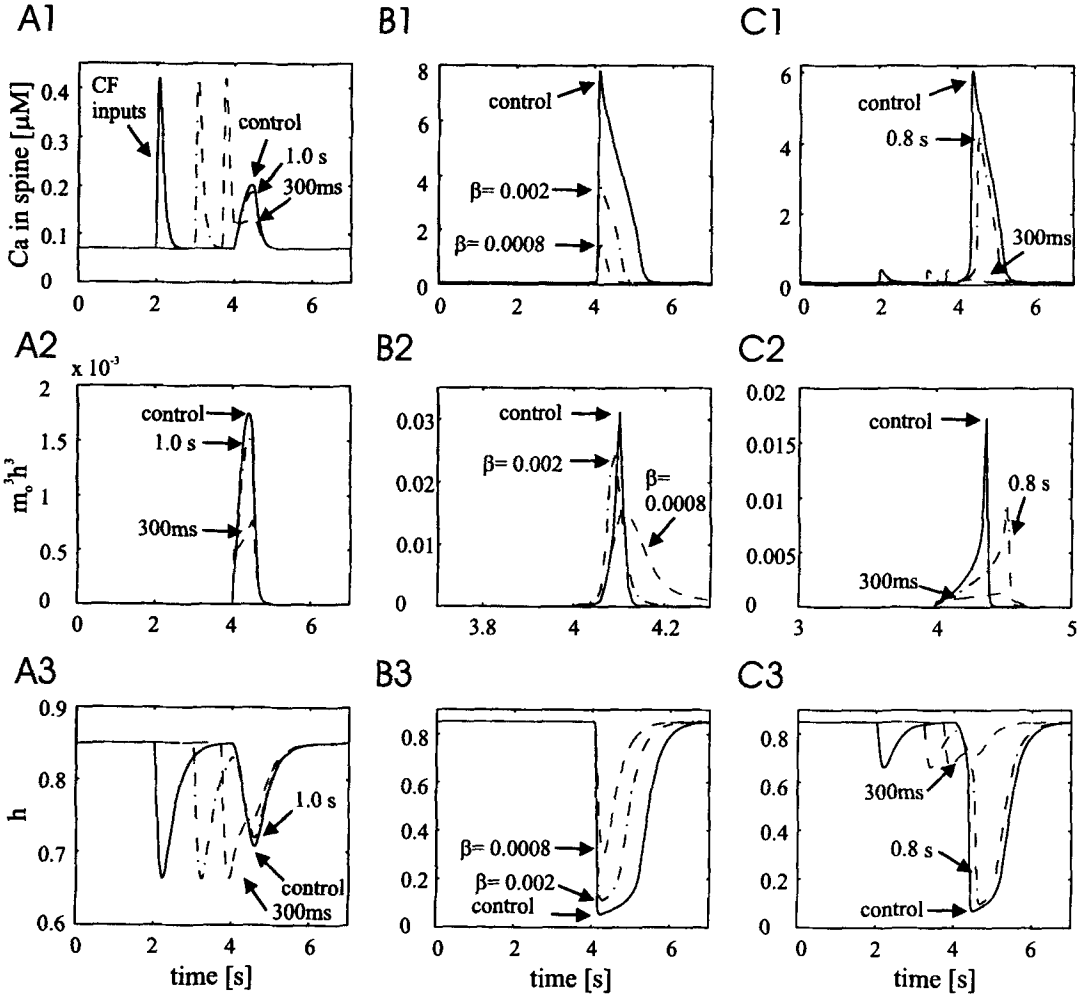

FIG. 4. The modulation of IICR by Ca^{2+} elevation. (A) the behavior of IICR induced by an IP_3 pulse (9.5 μM) at time 4 s, when a CF pulse is given several seconds before (control), 1 s or 300 ms before the IP_3 pulse. (A1) spine Ca^{2+}, (A2) conductance and (A3) inactivation. When the Ca^{2+} input occurs less than 1 s before the IP_3 increase, the IICR is diminished because the Ca^{2+} dependent inactivation is still present at the onset of the IP_3 pulse. (B) Effect on IICR when the CF input is given 50 ms after the IP_3 pulse. A large response results because the fast activation (m_0) is also Ca^{2+} dependent. When the relative conductance increases (B2) more Ca^{2+} is released (B1) which in its turn leads to increased conductance in a positive feedback manner until the Ca^{2+} dependent inactivation occurs (B3). The regenerative feedback response is diminished when the fraction of free Ca^{2+} is prevented from rising during this process as shown by using two different β values, 0.002 or 0.0008. The value of 0.0008 corresponds to the approximate β value during a subthreshold IP_3 pulse as in A. (C) IICR induced by suprathreshold IP_3 pulse (12 μM) is modulated by CF timing. The IP_3 pulse by itself leads to a large enough IICR to saturate the Ca^{2+} buffering system. The Ca^{2+} signal can be prevented by a Ca^{2+} elevation occurring 300 ms before.

elevation is further illustrated in Figure 4, which simulates IP_3 uncaging experiments. IP_3 is increased at time 4 s, and starts to decay after another half a second in all panels. In Figure 4A the IP_3 amplitude is under the threshold giving rise to a small Ca^{2+} signal (Fig. 4A1; control). In Figures 4A2 and 4A3 the relative IP_3 receptor conductance, corresponding to $m_0^3 \cdot h^3$ (see methods) and inactivation, h, are plotted. The amplitude of the Ca^{2+}

response following the IP_3 pulse is modulated when a CF input is given. If the CF input comes 1 s before the IP_3 increase, there is a small reduction in IICR compared to the control in which the CF input arrives several seconds before. When the CF input occurs 300 ms before the IP3 increase the response is further reduced. The underlying mechanism is a Ca^{2+} dependent inactivation (h decreases) of the IP_3 receptor (Khodakhah & Ogden, 1995), with a time constant that decreases with increased Ca^{2+} (see methods).

Figure 4B illustrates that, if the Ca^{2+} elevation is given after the IP_3 increase but before the inactivation has occurred, an amplification in Ca^{2+} concentration occurs. The conductance rises rapidly to higher values (Fig. 4B2) because the activation (m_0) is dependent both on IP_3 and Ca^{2+}. This increases IICR fast which in its turn leads to a rapid increase in conductance in a regenerative process. The unique buffering properties of Purkinje cells play a role in amplification of the IICR since the high affinity buffer saturates at around 1μM of Ca^{2+}; thus when the Ca^{2+} concentration increases above this level, the fraction of free Ca^{2+} is increased (see Maeda et al. 1999). The effect of buffer saturation is further illustrated by keeping β (the fraction of free Ca^{2+}) constant at two different values. A high value of β (0.002) results in a higher conductance and Ca^{2+} elevation compared to a lower β (0.0008). But preventing buffers from saturating by keeping β constant at either value reduces the Ca^{2+} increase due to IICR.

Figure 4C shows that the response to a suprathreshold IP_3 pulse, i.e., an IP_3 pulse that by itself produces enough Ca^{2+} release to saturate the buffering system, is modulated in the same way as the response to a subthreshold IP_3 pulse. However, the effect of a Ca^{2+} elevation occurring just before the IP3 increase is quantitatively more significant with respect to the differences in Ca^{2+} levels. In the model the IICR produced by the IP_3 pulse alone (Control) is clearly reduced when a single CF input is given 0.8 s before the IP_3 pulse due to the inactivation (Fig. 4C3) of the calcium release channel. This shows that IICR is modulated significantly by prior Ca^{2+} elevations, which is in accordance with in vitro measurements (Khodakhah & Ogden, 1995). More notably, a CF pulse given 300 ms before the IP_3 pulse dramatically reduces the calcium elevation to the extent that Ca^{2+} buffers are not saturated.

PKC temporal sensitivity

The production of active PKC is sensitive to ISI, as shown in Figure 5 which illustrates the amount of transiently and persistently active PKC in response to paired stimuli (CF follows PF by 250 ms) and unpaired stimuli (CF and PF are separated by 15 s) during a 30 s interval. Sensitivity to ISI is due to the activation requirements of PKC. The formation of transient PKC requires overlap of Ca^{2+} and DAG elevations. If CF activation occurs before PF activation, the Ca^{2+} transient has decayed prior to DAG elevation and minimal transient PKC builds up. If the CF input, instead, comes some time after the PF activation, an increase in tPKC occurs since the Ca^{2+} and DAG elevations partly overlap. Finally, long ISIs do not produce elevated tPKC because the Ca^{2+} signal occurs after the DAG signal has decayed. Since tPKC depends on an increase in calcium, sensitivity of tPKC to ISI is partly due to sensitivity of IICR to ISI. The formation of persistently active PKC requires temporal overlap in the tPKC and AA elevations. Thus, any conditions which do not produce tPKC elevation will not produce pPKC elevation. Furthermore, even if tPKC is elevated, if the AA increase has no temporal overlap with tPKC (i.e., AA increase is too early or too late) little pPKC is formed.

The mechanisms contributing to PKC sensitivity to ISI are further explored in Figure 6,

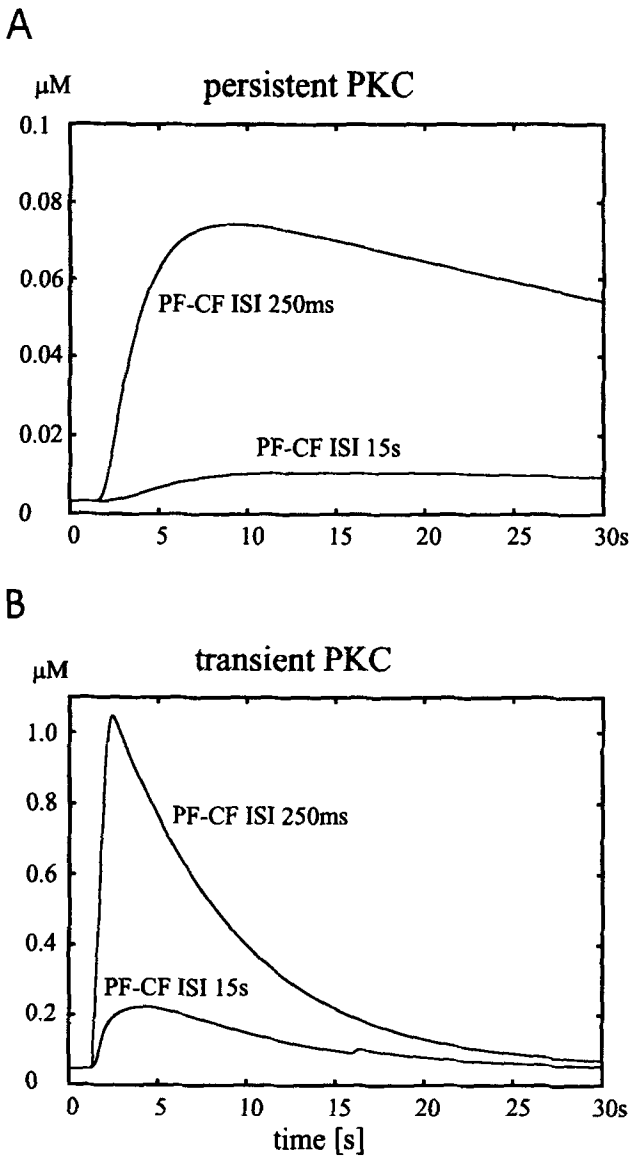

FIG. 5. Dynamics of persistent (A) and transient forms (B) of PKC following 8 PF and 3 CF (Schreurs, Oh & Alkon, 1996) with an interstimulus interval of either 250 ms (forward pairing) or 15 s (independent PF and CF activation pattern). Note that the dynamics of pPKC formation are slower than the dynamics of tPKC.

which summarizes the amount of tPKC, AA, and pPKC formation as a function of ISI. Note that pPKC in these simulations reaches a "steady-state" level after five to ten 30 s trials, with maximal values 2–2.5 times those reached after the first 30 s trial. In the full model (Fig. 6A), up to a tenfold increase relative to rest level of persistently formed PKC occurs when a PF input is followed by a CF input within a certain time window. When no IICR is included (Fig. 6B, circles), the Ca^{2+} elevation is only due to CF activation and thus there are no cooperative effects between different Ca^{2+} sources. Consequently, the pPKC

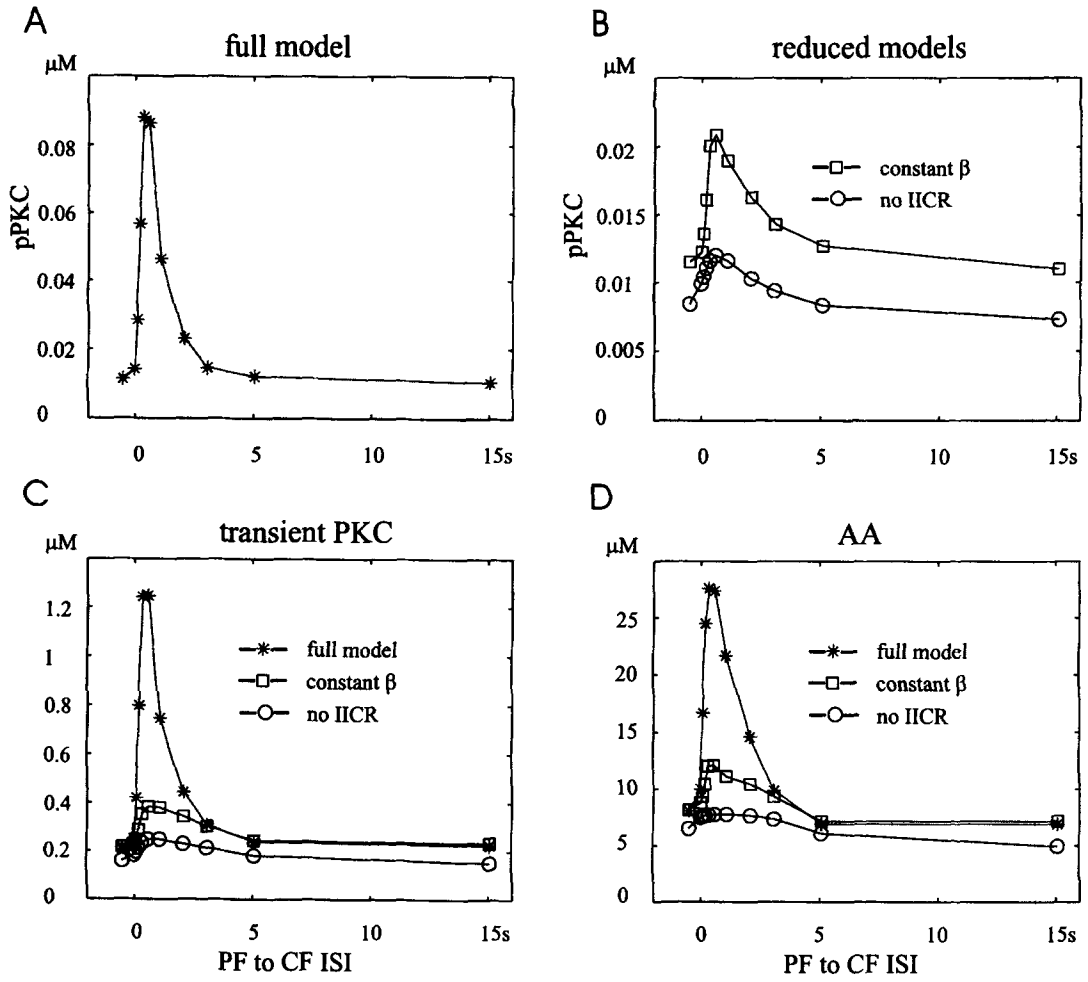

FIG. 6. Effect of ISI on PKC activation. ISI is indicated as time in seconds between the onset of 8 PF pulses and the onset of 3 CF pulses. Peak levels are shown after one 30s interval. (A) pPKC (B) pPKC in reduced models in which IICR is neglected (circles) or Ca^{2+} buffers are assumed to be nonsaturating (ß constant) (squares). The highest relative increase in pPKC is seen in the full model having both Ca^{2+} buffering and IICR. If the nonsaturating buffer is used instead (β=0.0008), the Ca^{2+} amplification is markedly reduced even though some facilitatory effects in the IP_3 Ca^{2+} release is seen when the CF Ca^{2+} pulses arrive. (C) tPKC and (D) AA formation for the different models. Note that the AA production depends on Ca^{2+} level as well as on DAG. Therefore the facilitatory effect of DAG on aPLA_2 increases the AA production more when the CF input is given when the DAG level is high (signaling that a PF input has arrived just before).

response is much reduced: without IICR, the increase of pPKC in response to the optimal ISI is only 50% greater than pPKC in response to unpaired (15 s ISI) stimuli. The ISI sensitivity of pPKC formation in this reduced model is due to the requirement for overlap of elevated levels of tPKC (Fig. 6C, circles) and AA (Fig. 6D, circles). The AA and tPKC peaks are much broader than the Ca^{2+} peak, and, thus the lesser sensitivity to ISI. If the fraction of free Ca^{2+} is kept constant (implying no saturation of buffers) but IICR is present, the production of pPKC in response to the optimal ISI is approximately twice that in response to unpaired stimuli (Fig. 6B, squares). The increase in pPKC is larger than in

the model with no IICR due to the small facilitatory effect on IICR when the CF Ca^{2+} elevation occurs in the critical time window (see Figure 3B). Since buffers are not saturated, the fraction of free Ca^{2+} is constant and will not facilitate the IICR in the strong regenerative fashion seen with the full model. In summary, the most important mechanism contributing to the production of pPKC is the interaction between IICR and CF induced Ca^{2+} in the presence of the Purkinje cell Ca^{2+} buffering properties; however, the dynamics of tPKC and AA also are significant.

DAG and AA decay

Because decay of AA and DAG are poorly constrained by biochemical experiments, the sensitivity of the model to variation of these parameters is evaluated. In Figure 7, PKC versus ISI is measured with the DAG (Fig. 7A) and AA (Fig. 7B) decay rates increased or decreased by a factor of five. To enhance comparison of the effect of parameters on the width of the ISI curves, the values for pPKC are scaled between 100% (for the optimal ISI) and 0% (for the base level of pPKC in response to unpaired inputs). Figures 7A1 and 7B1 show the sensitivity of the full model; Figures 7A2 and 7B2 show the sensitivity of the model with no IICR; and Figures 7A3 and 7B3 show the sensitivity of the model with non-saturating buffers. As seen in Figure 7B, AA decay has very little effect on sensitivity to ISI. The ISI curves for a 5-fold increase or 5-fold decrease in AA decay overlap the curve generated with default parameters. In contrast, a decrease in DAG decay rate reduces the sensitivity to ISI by increasing the forward ISIs that support elevation of pPKC. It is important to emphasize that in no case does a decrease in DAG decay result in pPKC elevation with backward ISIs. A second effect of DAG decay is seen in the models with no IICR (Fig. 7A2) and non-saturating buffers (Fig. 7A3). A smaller DAG decay shifts the optimal ISI from 0.5 s to 2 s.

In addition to the effect on the width of the ISI curves, DAG and AA decay rates have an effect on the relative amplitude increase of pPKC above the base level (the response to unpaired PF and CF stimulation) (Fig. 8). In the full model, the relative increase of pPKC during the optimal ISI is around 750%. It is diminished when DAG decay rate is reduced and is enhanced when the DAG decay rate is increased. Without IICR or with non-saturating buffers, changes in relative peak values are much smaller, but show a similar behavior when a change in decay rates is made. This further illustrates that saturating buffers and IICR ensure a high relative pPKC increase even when the decay rate of DAG is significantly increased. Similar to the effect of DAG decay, a change in AA decay produces a change in the relative increase in pPKC at the optimal ISI. A smaller AA decay rate decreases the relative increase of pPKC, and a larger AA decay increases the relative increase of pPKC. In summary, a change in AA or DAG decay rate has a minimal effect on temporal sensitivity of pPKC. However, the relative increase of pPKC at the optimal ISI is affected by AA and DAG decay rate.

Conventional LTD protocol

Figure 9 illustrates the pPKC, tPKC, and AA levels if a conventional LTD paradigm is used, i.e., low frequency (e.g. 1 Hz) activation of PF and CF. The same model parameters are used for LTD as for classical conditioning above; only the activation pattern of PF and CF inputs are changed. Sensitivity to ISI is low in the full model (Fig 9A, stars and 9B) and non-existent in the model with no IICR (Fig 9A, circles and 9C). A 1 Hz stimulation

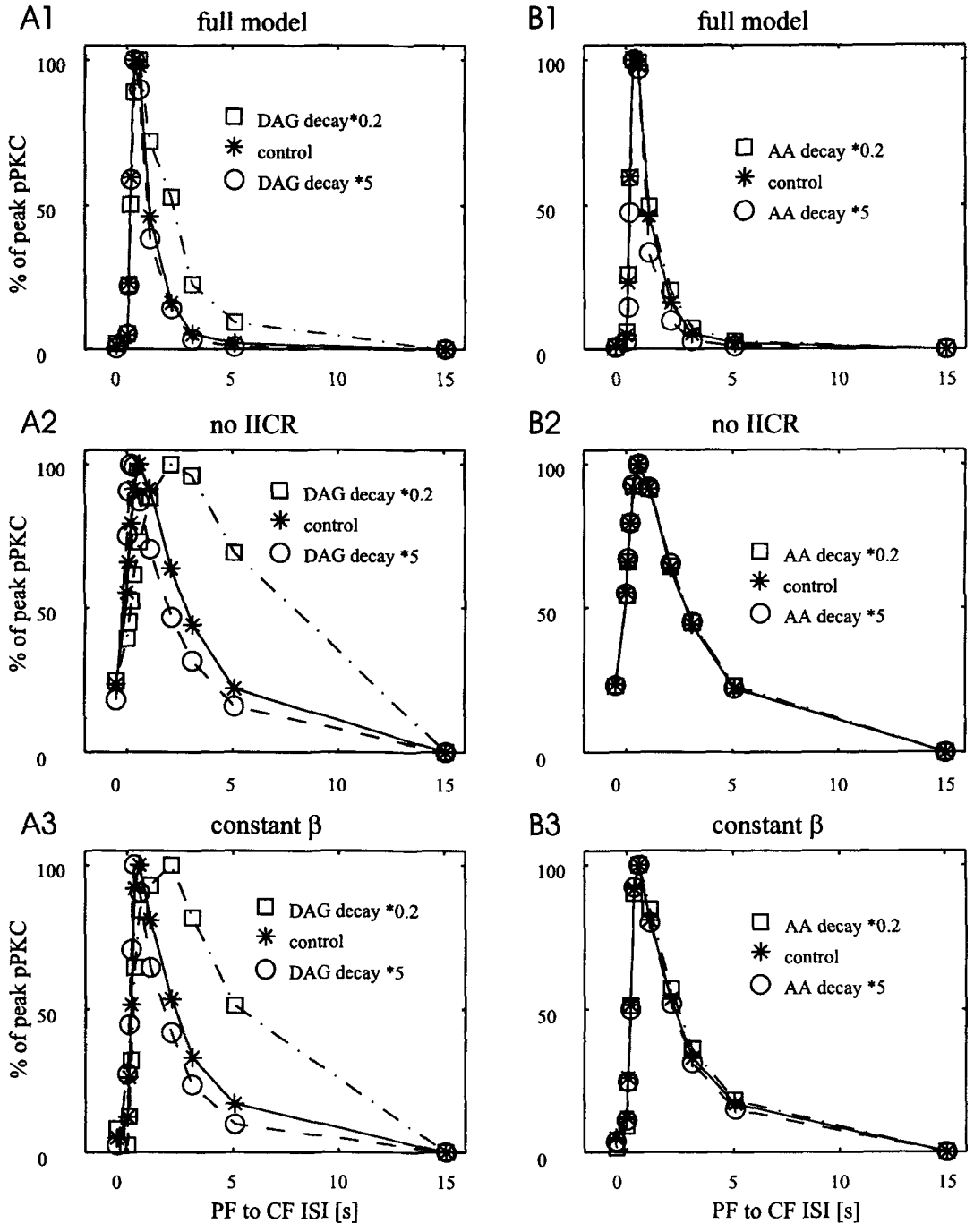

FIG. 7. The importance of the DAG (A) and AA (B) decay on ISI. In both the full model, the model lacking IICR or the model using nonsaturating Ca^{2+} buffers, the AA decay does not change the temporal sensitivity (B), but decreasing DAG decay delays and prolongs the interval in which a significant increase of pPKC is formed (A). Note that in the full model the dynamics of the interaction of CF Ca^{2+} and IICR increase significantly the robustness to variations of the DAG decay.

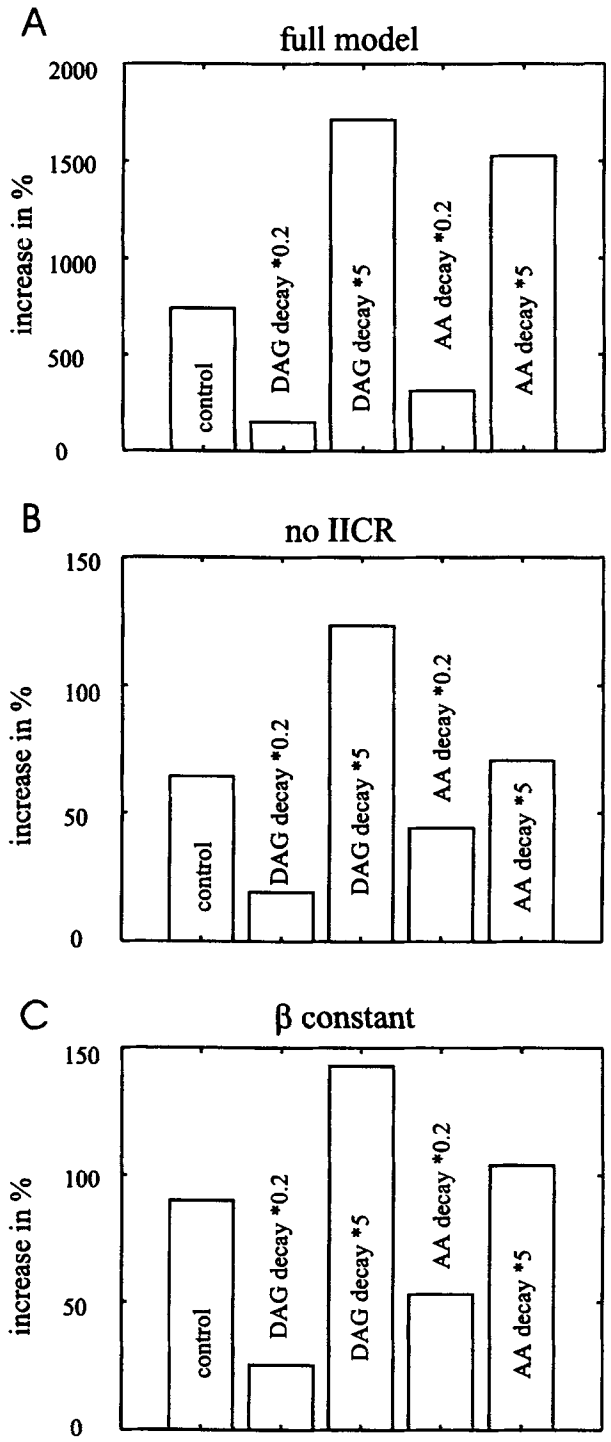

FIG. 8. DAG and AA decay rates affect the relative increase in peak pPKC concentration (pPKC at optimal ISI –pPKC for ISI 15s)/(pPKC for ISI 15 s). With increasing half lives of DAG or AA the peak pPKC response decreases. The effect of DAG and AA decay is smaller in the full model (A) as compared to the model with no IICR (B) and the model with ß constant (C).

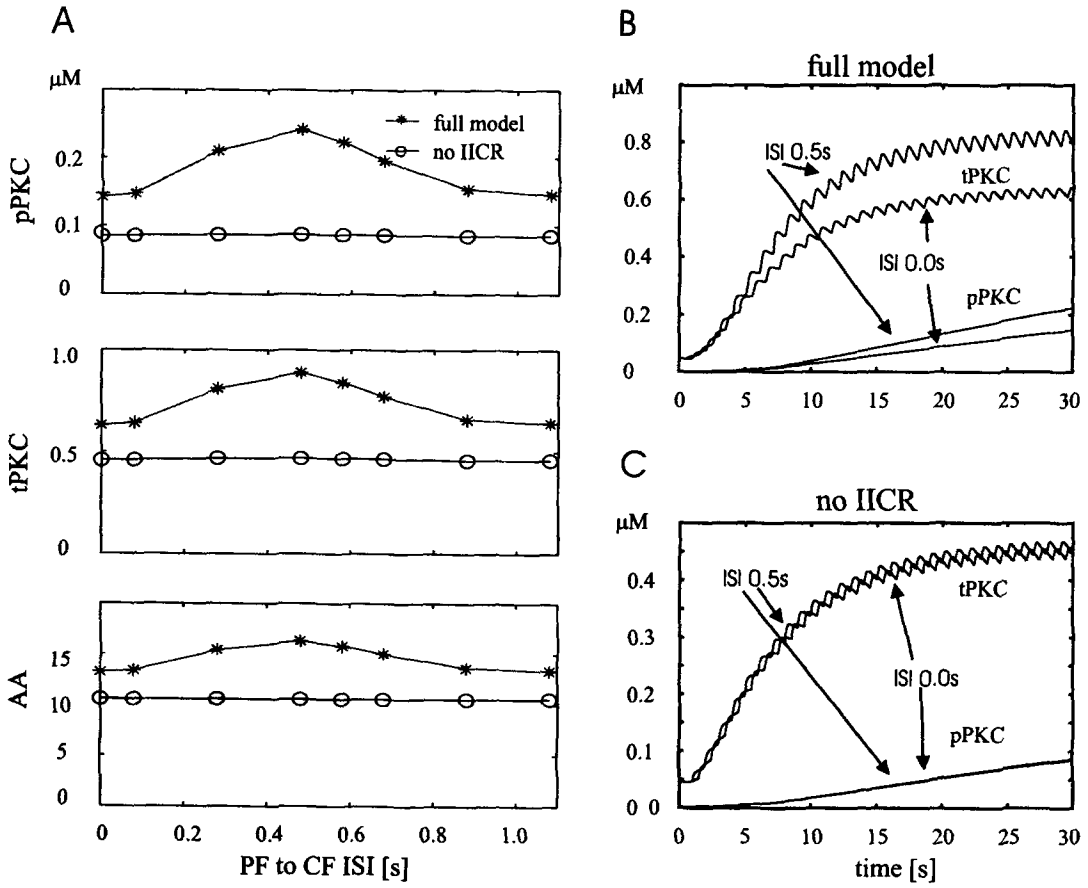

FIG. 9. Model simulations using a conventional LTD stimulation protocol (1 Hz PF and CF stimulation). (A) Effect of ISI on pPKC, tPKC and AA in full model (stars) and model with no IICR (circles). (B) Dynamics of tPKC and pPKC build up in full model. (C) Dynamics of tPKC and pPKC in model with no IICR.

rate is similar to the DAG and AA decay rates; thus, the concentration of these PKC activators remains elevated during the entire 1 s intertrial interval. Only the concentrations of Ca^{2+} and IP_3 fluctuate significantly during the intertrial interval. However, one Hz CF stimulation rates produce a fairly persistent increase in Ca^{2+}, which causes a partial ongoing inhibition of IICR in the model (see also Khodakhah & Ogden, 1995). An additional effect, not taken into account in the present model due to lack of quantitative data, is that AA inhibits the IP_3 receptor (Striggow & Ehrlich, 1997) which would further diminish the role of IICR in 1 Hz and faster repetitive CF activation due to a constant elevation of AA concentration.

Extended PF stimulation

Figure 10 investigates the consequences of using longer PF and CF trains. A significant formation of persistent PKC is achieved when a longer PF train is applied with an intertrial interval of 30 s, irrespective of whether it is combined with a CF input or not: approxi-

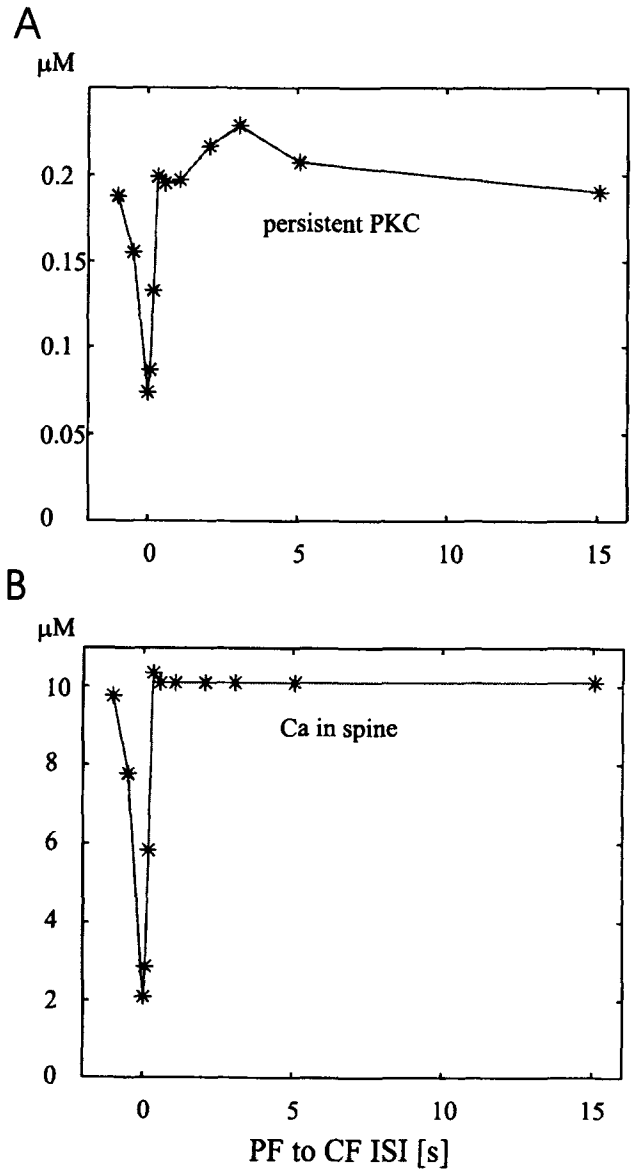

FIG. 10. Maximal levels of persistently formed PKC (A) and Ca^{2+} (B) when 40 PF pulses are combined with 10 CF as used by Schreurs and Alkon (1993). A dip in the maximal Ca^{2+} amplitude is seen when the CF input comes right before or simultaneously with the PF train due to Ca^{2+} dependent inactivation of the IICR.

mately the same amounts of pPKC are produced with a long PF train alone as with 8PF + 3CF. For most ISIs, the train of 40 PF activates IICR sufficiently to saturate the Ca^{2+} buffers and produce a large Ca^{2+} elevation in the spine (Fig 10B) and a prolonged elevation in DAG and AA. These results are in accordance with experimental results by Schreurs & Alkon (1993) that show that LTD is achieved with such long PF trains irrespective of whether they are combined with CF inputs or not (see also Hartell 1996). However, a reduction in the amount of pPKC is seen if a CF input is applied just before or

during the PF train (pPKC= 0.07 at 0 s). Interestingly, when a long PF train is applied to the model with no IICR, the peak pPKC is 0.0094 μM, suggesting that induction of LTD with PF alone requires IICR unless PF stimulation is strong enough to evoke dendritic Ca^{2+} spikes.

Discussion

PKC in classical conditioning

The aim of the present simulations was to evaluate the mechanisms underlying the temporal requirements of the conditioned stimulus (PF) and the unconditioned stimulus (CF) in memory storage in the cerebellum during classical conditioning. We asked to what extent this can be accounted for by the activation requirements of PKC following the arrival of PF and CF inputs in Purkinje cells. Our modeling of Purkinje cell biochemistry was guided by the myriad studies investigating the phenomenon of LTD observed in Purkinje cells in response to paired PF-CF stimulation. LTD is commonly believed to be a memory storage mechanism, but most LTD studies use intertrial intervals and interstimulus intervals that are incompatible with those that produce classical conditioning (Chen & Thompson, 1995; Schreurs, Oh & Alkon, 1996). To address this issue, Schreurs et al. (1996) developed a stimulation protocol that is compatible with classical conditioning; it used an 80 ms interstimulus interval and a 20–40 s intertrial interval. This "pairing specific" LTD was produced only with paired stimuli and not in response to PF or CF alone. Our simulations used this PSD protocol because it resembles classical conditioning protocols.

The results show that elevated PKC levels require a forward ISI between PF and CF input of approximately 0.1–3 s. This behavior is an emergent property of the model since the signaling of the respective PF and CF pathways were added independently of each other. Because of the similarities between the PSD stimulation protocol and classical conditioning protocols, we argue that the results observed in our study are similar to what would be observed in Purkinje cells in response to tone and puff stimuli. Thus, it seems appropriate to compare the ISI sensitivity of model PKC with ISI sensitivity of classical conditioning behavior. Figure 11 summarizes the data from Gormezano (1983) and illustrates the similarity of this data to the modeling results. There are two mechanisms whereby PKC activation leads to the behavioral response. First, PKC phosphorylation of AMPA receptors leads to synaptic depression (Lüscher, Nicoll, Malenka & Muller, 2000; Wang & Linden, 2000), which may be correlated with the decreased firing observed in some Purkinje cells (Berthier & Moore, 1986). Second, PKC may phosphorylate the transient potassium channel, leading to a reduction in this current and an increased Purkinje cell excitability as observed *in vitro* (Schreurs, Tomsic, Gusev & Alkon, 1997) and *in vivo* (Berthier & Moore, 1986) after classical conditioning.

Our model assumes that the granule cell response to a tone is an 80 ms burst of spikes at the tone onset. This does not imply that an ISI greater than 80 ms corresponds to trace conditioning. Rather, the 80 ms spike burst is consistent with the brief granule cell activity observed in response to tactile stimulation (Brown & Bower, 2001; Gunduppa-Sulur, De Schutter & Bower, 1999), and with the spike frequency adaptation observed in the auditory system. An alternative is to model the granule cell response to a tone as an initial burst of spikes followed by a lower frequency activity for the duration of the tone. This PF stimulation would clarify the analogy to delay conditioning, and should improve the similarity of

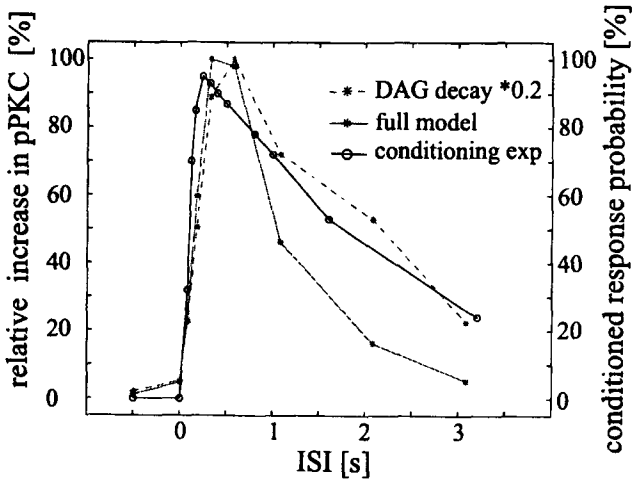

FIG. 11. Comparison between formation of persistently active PKC in the present model, expressed as percentage of peak amplitude, and conditioned response probability following classical conditioning (data replotted from Gormezano, Kehoe & Marshall, 1983).

PKC activation to the behavioral data. Prolonged PF activity would increase DAG concentration and PKC activity for longer ISIs, similar to the effect of decreasing DAG decay (Fig 11: dashed line). But, in contrast to the effect of decreasing DAG decay, prolonged granule cell activity for long tones would not affect the PKC peak at short ISIs. The CF input used by Schreurs, Oh & Alkon (1996) is slightly higher than the CF frequencies observed during physiological circumstances, e.g., 10 Hz (Lang, Sugihara, Welsh & Llinas, 1999). The use of a lower CF frequency would not change the temporal sensitivity of IICR, although a small change in the amplitude of the AA signal may result.

Calcium dynamics and ISI sensitivity

An unanticipated result was that the amplitude of Ca^{2+} elevation was sensitive to the ISI of PF and CF stimulation. The calcium concentration reached 6–8 μM if PF preceded CF by 300 ms, but was only 1 μM if CF preceded PF by 300 ms. This sensitivity to ISI was due to the effect of Ca^{2+} on the IP_3 receptor channel. Simulations showed that IICR was facilitated by a transient Ca^{2+} elevation if it occurred during the early phase of IP_3 elevation before IICR had become inactivated. IICR was inhibited by a transient CF induced Ca^{2+} elevation if it occurred less than 1 s prior to IP_3 elevation.

The unique buffering system of Purkinje cells interacts with properties of the IP_3 receptor channel to produce the dramatic sensitivity to ISI. When the high affinity buffer becomes saturated, the free Ca^{2+} increases more rapidly and facilitates calcium release. The buffering system has an apparent threshold around 1 μM and above this free Ca^{2+} concentration a supralinear summation between the different Ca^{2+} sources occurs as discussed in Maeda, Ellis-Davies, Ito, Miyashita & Kasai (1999). This threshold also implies that smaller perturbations below this threshold can be discarded, e.g., single or random PF and CF inputs.

Calcium in Purkinje cell dendrites is strongly regulated by GABA inhibitory synaptic

inputs (Midtgaard, 1995). Accordingly, the vast majority of LTD experiments conducted in slice preparations block fast GABAergic synaptic transmission because GABA activation following CF stimulation (which is typically presented prior to PF stimulation) prevents LTD induction. In classical conditioning protocols, PF is presented first, and the calcium elevation which occurs rapidly following CF stimulation probably precedes the multisynaptic GABAergic activation. Even if CF dependent Ca^{2+} entry is still affected by GABAergic inputs, this is not critical since the CF evoked Ca^{2+} signal just needs to be large enough to facilitate the IICR. Ca^{2+} dependent potentiation of GABAergic signals (Marty & Llano, 1995) also is not an issue in a classical conditioning paradigm because of the long intertrial interval, allowing for complete decay of inhibitory signals prior to subsequent PF-CF stimuli. This interpretation is in accordance with experiments which show that LTD can be evoked experimentally without GABA blockers when using trains of PF inputs followed by a CF input (Schreurs, Oh & Alkon, 1996; Wang, Denk & Hausser, 2000).

Model predictions

These results on Ca^{2+} behavior predict that Ca^{2+} elevation in Purkinje cell spines is sensitive to PF-CF stimulation interval. This prediction has recently been evaluated and confirmed by Wang, Denk & Hausser (2000) (see also Nakamura, Barbara, Nakamura & Ross, 1999). Our results, however, further suggest that Ca^{2+} buffers are necessary for this behavior in Purkinje cells.

The temporal behavior of the model is robust to variations in AA decay rate. In contrast, decreasing the DAG decay rate delays the optimal ISI and increases the range of ISI that support PKC activation. This sensitivity to DAG decay rate is due to PKC dynamics because facilitation of IICR is independent of DAG decay rate. Consequently, an important prediction of the model is that DAG decay rate is on the order of several per second. In this context it is interesting that diacylglycerol kinase is especially high in spines (Goto & Kondo, 1999). Since the DAG decay rate has not yet been measured, this is an untested prediction of the model.

Because the biochemical pathways activated by PF and CF stimulation (see Daniel, Levenes & Crepel, 1998; Levenes, Daniel & Crepel, 1998 for reviews) are the same for LTD and PSD, using an LTD stimulation protocol (e.g., a 1 s intertrial interval) also should lead to an increase in PKC, as demonstrated by Kuroda, Schweighofer & Kawato (2001). We tested this prediction using various ISIs. The results showed that this conventional LTD protocol produced an elevation in PKC that was relatively insensitive to ISI. Thus the model predicts that sensitivity to ISI in LTD is not mediated by PKC, but by some other as yet unidentified substance. This may be related to the observation that ISI sensitivity is not consistent between different LTD protocols (Chen & Thompson, 1995; Ekerot & Kano, 1989; Karachot, Kado & Ito, 1994).

LTD has been induced with either a large increase in DAG alone or a Ca^{2+} elevation alone (Finch & Augustine, 1998; Narasimhan, Pessah & Linden, 1998; see also Schreurs & Alkon, 1993). Model simulations evaluated this observation using a long (40 PF pulses) stimulation protocol. The results showed that extended PF stimulation activated pPKC regardless of whether it was combined with a CF input, due to activation of IICR. This leads to the prediction that blocking IICR will prevent LTD induction by PF alone, a prediction that has not yet been tested.

Interaction among second messenger pathways

Our results complement other studies showing that pattern of activation is critical in determining which enzyme or what quantity of enzymes are activated. Pattern of activation refers to all the temporal aspects describing synaptic inputs such as the number of synaptic inputs (Holmes, 2000) or the frequency of synaptic inputs (Bhalla, 2000). Our work resembles that of Bhalla & Iyengar (1999) and Kuroda, Schweighofer & Kawato (2001) in that both show that two different biochemical pathways may interact to produce an emergent behavior that is not present in any of the pathways alone. However, in our model, in contrast to theirs, the emergent behavior depends on the relative timing of the activation of the biochemical pathways.

Our model excludes two signalling pathways: NO to PKG, and MAPK which may play a role in LTD or classical conditioning. NO may be released by PF activation (Bredt, Hwang & Snyder, 1990; Southam, Morris & Garthwaite, 1992) and diffuse into nearby Purkinje cells activating the cGMP, PKG pathway, one consequence of which is to inactivate phosphatases. LTD/PSD and excitability changes (Schreurs, Tomsic, Cusev & Alkon, 1997) thus may be promoted by both phosphorylation by the PKC pathway and inhibition of dephosphorylation by the NO pathway (Levenes, Daniel & Crepel, 1998). The NO pathway was not modeled because it is unknown whether it contributes *in vivo* to the temporal sensitivity during classical conditioning.

MAPK, which has been found to be partly but not fully activated in LTD, can influence the effective mGluR1 and PKC activation (Kawasaki, Fujii, Gotoh, Morooka, Shimohama, et al., 1999), and it also stimulates the PLA_2 enzyme (Qiu & Leslie, 1994). However, it is too slowly activated (Qiu & Leslie, 1994) to contribute to the temporal sensitivity of classical conditioning and thus not used in the present model. *In vivo,* it may be activated upon consecutive classical conditioning trials, and may be required to prolong and amplify the pPKC formation and other long-term changes (including protein synthesis) following learning, see Kuroda, Schweighofer & Kawato (2001).

In conclusion, our results present a cellular basis for ISI sensitivity and thus differs from other studies showing that ISI sensitivity is a property of networks of cells. Other models have assumed that granule cells (or the response of Purkinje cells to granule cells) have different time-dependent activity variations that are repeatable over trials (Fiala, Grossberg & Bullock, 1996; see Medina & Mauk, 2000 for a review). For example, following a CS, some PFs are active immediately following stimulus onset while some are not active until later following CS onset. LTD occurs at only those PF-Purkinje cell synapses that are active when the US input arrives (Medina, Garcia, Nores, Taylor & Mauk, 2000). These models assume that LTD requires a very narrow coincidence detection. Depression occurs when the CF and PF are active simultaneously. Our modeling of PKC, shown to be critical to LTD, suggests the coincidence detection is much broader. Thus, these network models will exhibit much broader ISI sensitivity if realistic biochemical interactions are included. Most likely, both network properties and subcellular properties of key enzymes are both responsible for ISI sensitivity.

Acknowledgments

J. Hellgren Kotaleski was supported by the Knut and Alice Wallenbergs Foundation. K.T. Blackwell was supported by NIH grant K21-MH01141 and NSF grant IBN–0077509.

References

Allbritton, N. L., Meyer, T., & Stryer, L. (1992). Range of messenger action of calcium ion and inositol 1,4,5-trisphosphate. *Science,* 258, 1812–1815.

Berthier, N. E. & Moore, J. W. (1986). Cerebellar purkinje cell activity related to the classically conditioned nictitating membrane response. Exp *Brain Res,* 63, 341–350.

Bhalla, U. S. (2000). Temporal pattern decoding by synaptic signaling pathways. Soc. *for Neurosci. Abstr,* 26, 1903.

Bhalla, U. S. & Iyengar, R. (1999). Emergent properties of networks of biological signaling pathays. *Science,* 283, 381–387.

Bramham, C. R., Alkon, D. L., & Lester, D. S. (1994). Arachidonic acid and diacylglycerol act synergistically through protein kinase C to persistently enhance synaptic transmission in the hippocampus. *Neuroscience,* 60, 734–743.

Bredt, D. S., Hwang, P. M., & Snyder, S. H. (1990). Localization of nitric oxide synthase indicating a neural role for nitric oxide. *Nature,* 347, 768–770.

Brown, I. E. & Bower, J. M. (2001). Congruence of mossy fiber and climbing fiber tactile projections in the lateral hemispheres of the rat cerebellum. *J. Comp. Neurol,* 429, 59–70.

Callaway, J. C., Lasser-Ross, N., & Ross, W. N. (1995). IPSPs strongly inhibit climbing fiberactivated [Ca 2+ji increases in the dendrites of cerebellar Purkinje neurons. *J. Neurosci,* 15, 2777–2787.

Canepari, M., Papageorgiou, G., Corrie, J. E., Watkins, C., & Ogden, D. (2001). The conductance underlying the parallel fibre slow epsp in rat cerebellar purkinje neurones studied with photolytic release of I-glutamate. *J. Physiol,* 533, 765–72.

Chen, C. & Thompson, R. F. (1995). Temporal specificity of long-term depression in parallel fiber-purkinje synapses in rat cerebellar slice. *Learning and Memory,* 2 185–198.

Daniel, H., Levenes, C., & Crepel, F. (1998). Cellular mechanisms of cerebellar LTD. *Trends in Neurosciences,* 21, 401–407.

De Schutter, E. & Bower, J. M. (1994). An active membrane model of the cerebellar Purkinje cell. I. Simulation of current clamps in slice. J. *Neurophysiol,* 71, 375–400.

Destexhe, A., Mainen, Z. F., & Sejnowski, T. J. (1994). Synthesis of models for excitable membranes, synaptic transmission and neuromodulation using a common kinetic formalism. *J Comput Neurosci, 1,* 195–230.

Ekerot, C. F. & Kano, M. (1989). Stimulation parameters influencing climbing fibre induced long-term depression of parallel fibre synapses. *Neurosci. Res,* 6 264–268.

Fiala, J. C., Grossberg, S., & Bullock, D. (1996). Metabotropic glutamate receptor activation in cerebellar Purkinje cells as substrate for adaptive timing of the classically conditioned eye-blink response. J. *Neurosci,* 16, 3760–3774.

Finch, E. A. & Augustine, G. J. (1998). Local calcium signalling by inositol–1,4,5-trisphosphate in Purkinje cell dendrites. *Nature,* 396, 753–756.

Freeman Jr, J. H., Schaarenberg, A. M., Olds, J. L., & Schreurs, B. G. (1998). Classical conditioning increases membrane-bound protein kinase C in rabbit cerebellum. *NeuroReport,* 9, 2237–2241.

Freeman Jr, J. H., Shi, T., & Schreurs, B. G. (1998). Pairing-specific long-term depression prevented by blockade of PKC or intracellular Ca^{2+}. *NeuroReport,* 9, 2237–2241.

Gormezano, I., Kehoe, E. J., & Marshall, B. S. (1983). Twenty years of classical conditioning research with the rabbit. *Prog Psychobiol and Physiol Psych,* 10, 197–275.

Goto, K. & Kondo, H. (1999). Diacylglycerol kinase in the central nervous system-molecular heterogeneity and gene expression. *Chem Phys Lipids,* 98, 109–117.

Gould, T. J. & Steinmetz, J. E. (1996). Changes in rabbit cerebellar cortical and interpositus nucleus activity during acquisition, extinction, and backward classical eyelid conditioning. *Neurobiology of Learning and Memory,* 65, 17–34.

Green, J. T. & Woodruff-Pak, D. S. (2000). Eyeblink classical conditioning: hippocampal formation is for neutral stimulus associations as cerebellum is for association-response. *Psychol Bull,* 126, 138–158.

Gruart, A., Guillazo-Blanch, G., Fernandez-Mas, R., Jimenez-Diaz, L., & Delgado-Garcia, J. M. (2000). Cerebellar posterior interpositus nucleus as an enhancer of classically conditioned eyelid responses in alert cats. *J. Neurophysiol,* 84, 2680–90.

Gunduppa-Sulur, G., De Schutter, E., & Bower, J. M. (1999). Ascending granule cell axon: an important component of cerebellar cortical circuitry. J. *Comp. Neur, 408,* 580–596.

Hartell, N. A. (1996). Strong activation of parallel fibers produces localized calcium transients and a form of LTD that spreads to distant synapses. *Neuron,* 16, 601–610.

Hemart, N., Daniel, H., Jaillard, D., & Crepel, F. (1995). Receptors and second messengers involved in long-term depression in rat cerebellar slices in vitro: a reappraisal. *Eur. J. Neurosci, 7,* 45–53.

Hirono, M., Konishi, S., & Yoshioka, T. (1998). Phospholipase C-independent group I metabotropic glutamate receptor-mediated inward current in mouse purkinje cells. *Biochem Biophys Res Commun,* 251, 753–8.

Hirono, M., Sugiyama, T., Kishimoto, Y., Sakai, I., Miyazawa, T., Kishio, M., Inoue, H., Nakao, K., Ikeda, M., Kawahara, S., Kirino, Y., Katsuki, M., Horie, H., Ishikawa, Y., & Yoshioka, T. (2001). Phospholipase cbeta4 and protein kinase calpha and/or protein kinase cbetai are involved in the induction of long term depression in cerebellar purkinje cells. J *Biol Chem,* 276, 45236–42.

Holmes, W. R. (2000). Models of calmodulin trapping and CaM kinase I activation in a dendritic spine. *J. Comput. Neurosci,* 8, 65–85.

Ivkovich, D., Paczkowski, C. M., & Stanton, M. E. (2000). Ontogeny of delay versus trace eyeblink conditioning in the rat. *Dev Psychobiol,* 36, 148–60.

Jafri, M. S. & Keizer, J. (1997). Agonist-induced calcium waves in oscillatory cells: a biological example of Burgers' equation. *Bull Math Biol,* 59, 1125–1144.

Kaftan, E. J., Ehrlich, B. E., & Watras, J. (1997). Inositol 1,4,5-trisphosphate (insp3) and calcium interact to increase the dynamic range of insp3 receptor-dependent calcium signaling. *J Gen Physiol,* 110, 529–538.

Kano, M., Garaschuk, 0., Verkhratsky, A., & Konnerth, A. (1995). Ryanodine receptormediated intracellular calcium release in rat cerebellar purkinje neurones. *J. Physiol,* 487, 1–16.

Karachot, L., Kado, R. T., & Ito, M. (1994). Stimulus parameters for induction of long-term depression in in vitro rat Purkinje cells. *Neurosci. Res,* 21, 161–168.

Katz, D. B. & Steinmetz, J. E. (1997). Single-unit evidence for eye-blink conditioning in cerebellar cortex is altered, but not eliminated, by interpositus nucleus lesions. *Learn Mem,* 4, 88–104.

Kawasaki, H., Fujii, H., Gotoh, Y., Morooka, T., Shimohama, S., Nishida, E., & Hirano, T. (1999). Requirement for mitogen-activated protein kinase in cerebellar long term depression. *J Biol Chem,* 487, 13498–13502.

Khodakhah, K. & Ogden, D. (1995). Fast activation and inactivation of inositol trisphosphate evoked Ca^{2+} release in rat cerebellar Purkinje neurones. *J. Physiol.,* 487, 343–358.

Kuroda, S., Schweighofer, N., & Kawato, M. (2001). Exploration of signal transduction pathways in cerebellar long-term depression by kinetic simulation. J. *Neurosci,* 21, 5693–702.

Lang, E. J., Sugihara, I., Welsh, J. P., & Llinas, R. (1999). Patterns of spontaneous Purkinje cell complex activity in the awake rat. J *Neurosci.,* 1 2728–2739.

Leslie, C. C. & Channon, J. Y. (1990). Anionic phospholipids stimulate an arachidonoyl-hydrolyzing phospholipase A_2 from macrophages and reduce the calcium requirement for activity. *Biochimica et Biophysica Acta,* 1045, 261–270.

Lester, D. S. & Bramham, C. R. (1993). Persistent, membrane-associated protein kinase C: from model membranes to synaptic long-term potentiation. *Cell Signal,* 5, 695–708.

Levenes, C., Daniel, H., & Crepel, F. (1998). Long-term depression of synaptic transmission in the cerebellum: cellular and molecular mechanisms revisited. *Progress in Neurobiology,* 55, 79–91.

Li, Y.-X. & Rinzel, J. (1994). Equations for InsP3 receptor—mediated $[Ca^{2+}]$i oscillations derived from a detailed kinetic model: a Hodgkin-Huxley like formalism. J. *Theor. Biol,* 166, 461–473.

Linden, D. J. (1995). Phospholipase A2 controls the induction of short-term versus long-term depression in the cerebellar Purkinje neuron in culture. *Neuron,* 15, 1393–1401.

Lüscher, C., Nicoll, R. A., Malenka, R. C., & Muller, D. (2000). Synaptic plasticity and dynamic modulation of the postsynaptic membrane. *Nat Neurosci,* 3, 545–550.

Maeda, H., Ellis-Davies, G. C., Ito, K., Miyashita, Y., & Kasai, H. (1999). Supralinear Ca^{2+} signaling by cooperative and mobile Ca^{2+} buffering in purkinje neurons. *Neuron,* 24, 989–1002.

Marty, A. & Llano, I. (1995). Modulation of inhibitory synapses in the mammalian brain. *Curr Opin Neurobiol,* 5, 335–41.

McCormick, D. A. & Thompson, R. F. (1984). Cerebellum: Essential involvement in the classically conditioned eyelid response. *Science,* 223, 296–299.

Medina, J. F., Garcia, K. S., Nores, W. L., Taylor, N. M., & Mauk, M. D. (2000). Timing mechanisms in the cerebellum: testing predictions of a large-scale computer simulation. *Neurosci,* 41, 5516–5525.

Medina, J. F. & Mauk, M. D. (2000). Computer simulation of cerebellar information processing. *Nat Neurosci,* 3, 1205–1211.

Midtgaard, J. (1995). Spatial synaptic integration in purkinje cell dendrites. J. Physiol *Paris,* 89, 23–32.

Miyakawa, H., Lev-Ram, V., Lasser-Ross, N., & Ross, W. N. (1992). Calcium transients evoked by climbing fiber and parallel fiber synaptic inputs in guinea pig cerebellar Purkinje neurons. *J. Neurophysiol.,* 68, 1178–1189.

Miyata, M., Finch, E. A., Khiroug, L., Hashimoto, K., Hayasaka, S., Oda, S. I., Inouye, M., Takagishi, Y., Augustine, G. J., & Kano, M. (2000). Local calcium release in dendritic spines required for long-term synaptic depression. *Neuron*, 28, 233–244.

Mukhopadhyay, S. & Ross, E. M. (1999). Rapid GTP binding and hydrolysis by G(q) promoted by receptor and GTPase-activating proteins. *Proc. Natl. Acad. Sci*, 96 9539–9544.

Nakamura, T., Barbara, J.-G., Nakamura, K., & Ross, W. N. (1999). Synergistic release of Ca^{2+} from IP_3-sensitive stores evoked by synaptic activation of mGluRs paired with backpropagating action potentials. *Neuron*, 24, 727–737.

Narasimhan, K., Pessah, I. N., & Linden, D. J. (1998). Inositol–1,4,5-trisphosphate receptor mediated Ca mobilization is not required for cerebellar long-term depression in reduced preparations. J *Neurophysiol*, 80, 2963–2974.

Netzeband, J. G., Parsons, K. L., Sweeney, D. D., & Gruol, D. L. (1997). Metabotropic glutamate receptor agonists alter neuronal excitability and ca2+ levels via the phospholipase c transduction pathway in cultured purkinje neurons. J *Neurophysiol*, 78, 63–75.

Oancea, E. & Meyer, T. (1998). Protein kinase C as a molecular machine for decoding calcium and diacylglycerol signals. *Cell*, 95, 307–318.

Pete, M. J. & Exton, J. H. (1996). Purification of a lysophospholipase from bovine brain that selectively deacylates arachidonyl-substituted lysophosphatidyl-choline. *J. Biol. Chemistry*, 271, 18114–18121.

Petit, K., De Block, J., & De Potter, W. (1995). Isolation and characterization of a cytosolic phospholipase A2 from bovine adrenal medulla. J. *Neurochemistry*, 41 139–146.

Qiu, Z.-H. & Leslie, C. C. (1994). Protein kinase C-dependent and-independent pathways of mitogen-activated protein kinase activation in macrophages by stimuli that activate phospholipase A_2 *J. Biol. Chem*, 269, 19480–19487.

Reynolds, T. & Hartell, N. A. (2001). Roles for nitric oxide and arachidonic acid in the induction of heterosynaptic cerebellar LTD. *Neuroreport*, 12, 133–136.

Ryon, J. W., Cho, S. Y., & Kim, H. T. (2001). Lesions of the entorhinal cortex impair acquisition of hippocampal-dependent trace conditioning. *Neurobiol Learn Mem*, 75, 121–7.

Sabatini, B. L., Maravall, M., & Svoboda, K. (2001). Ca2+ signaling in dendritic spines. *Current Opinion in Neurobiology*, 11, 349–356.

Schacter, J. B., Lester, D. S., & Alkon, D. L. (1996). Synergistic activation of protein kinase C by arachidonic acid and diacylglycerol in vitro: generation of a stable membrane-bound, cofactor—independent state of protein kinase C activity. *Biochimica et Biophysica Acta*, 1291, 167–176.

Schreurs, B. G. & Alkon, D. L. (1993). Rabbit cerebellar slice analysis of long-term depression and its role in classical conditioning. *Brain Res*, 631, 235–240.

Schreurs, B. G., Oh, M. M., & Alkon, D. L. (1996). Pairing-specific long-term depression of Purkinje cell excitatory postsynaptic potentials results from a classical conditioning procedure in the rabbit cerebellar slice. *J. Neurophysiol*, 75, 1051–1060.

Schreurs, B. G., Tomsic, D., Gusev, P. A., & Alkon, D. L. (1997). Dendritic excitability microzones and occluded long-term depression after classical conditioning of the rabbit's nictitating membrane response. *J. Neurophysiol*, 77, 86–92.

Shinomura, T., Asaoka, Y., Oka, M., Yoshida, K., & Nishizuka, Y. (1991). Synergistic action of diacylglycerol and unsaturated fatty acid for protein kinase C activation: its possible implications. *Proc. Natl. Acad. Sci*, 88, 5149–5153.

Shirai, Y., Kashiwagi, K., Yagi, K., Sakai, N., & Saito, N. (1998). Distinct effects of fatty acids on translocation of gamma—and epsilon-subspieces of protein kinase C. J. *Cell Biol*, 143, 511–521.

Shirai, Y., Sakai, N., & Satir, N. (1998). Subspieces-specific targeting mechanism of protein kinase C. *Jpn.* J. *Pharmacol*, 78, 411–117.

Smrcka, A. V., Hepler, J. R., Brown, K. 0., & Sternweis, P. C. (1991). Regulation of polyphosphoinositide-specific phospholipase C activity by purified Gq. *Science*, 251, 804–807.

Southam, E., Morris, R., & Garthwaite, J. (1992). Sources and targets of nitric oxide in rat cerebellum. *Neurosci Lett*, 137, 241–244.

Stanton, M. E. (2000). Multiple memory systems, development and conditioning. *Behav Brain Res*, 110, 25–37.

Steinmetz, J. E. (2000). Brain substrates of classical eyeblink conditioning: a highly localized but also distributed system. *Behav Brain Res*, 110, 13–24.

Stella, N., Pellerin, L., & Magistretti, B. J. (1995). Modulation of the glut amate-evoked release of arachidonic acid from mouse cortical neurons: involvement of a pH sensitive membrane phospholipase A2. J. *Neurosci*, 15, 3307–3317.

Striggow, F. & Ehrlich, B. E. (1997). Regulation of intracellular calcium release channel function by arachidonic acid and leukotriene B4. *Biochern Biophys Res Commun*, 237, 413–418.

Takechi, H., Eilers, J., & Konnerth, A. (1998). A new class of synaptic response involving calcium release in dendritic spines. *Nature*, 396, 757–760.

Tempia, F., Miniaci, C., Anchisi, D., & Strata, P. (1998). Postsynaptic current mediated by metabotropic glutamate receptors in cerebellar Purkinje cells. J. *Neurophysiol,* 80, 520–528.

Thompson, R. F. (1986). The neurobiology of learning and memory. *Science*, 233, 941–947.

Thompson, R. F. & Kim, J. J. (1996). Memory systems in the brain and localization of a memory. *Proc. Natl. Acad. Sci*, 93, 13438–13444.

Thompson, R. F. & Krupa, D. J. (1994). Organization of memory traces in the mammalian brain. *Ann. Rev. Neurosci.*, 17, 519–549.

Wang, S. S., Alousi, A. A., & Thompson, S. H. (1995). The lifetime of inositol 1,4,5-trisphosphate in single cells. J *Gen Physiol*, 105, 149–171.

Wang, S. S.-H., Denk, W., & Hausser, M. (2000). Coincidence detection in single dendritic spines mediated by calcium release. *Nat Neurosci*, 3, 1266–1273.

Wang, Y. T. & Linden, D. J. (2000). Expression of cerebellar long-term depression requires postsynaptic clathrin-mediated endocytosis. *Neuron*, 25, 635–647.

Watras, J., Bezprozvanny, I., & Ehrlich, B. E. (1991). Inositol 1,4,5-trisphosphate-gated channels in cerebellum: presence of multiple conductance states. J. *Neurosci*, 1 3239–45.

Watras, J., Orlando, R., & Moraru, I. 1. (2000). An endogenous sulfated inhibitor of neuronal inositol trisphosphate receptors. *Biochemistry*, 39, 3452–60.

Woodruff-Pak, D. S., Lavond, D. G., & Thompson, R. F. (1985). Trace conditioning: abolished by cerebelar nuclear lesions but not lateral cerebellar cortex aspiration. *Brain Res.*, 348, 249–260.

Yang, K., Hellgren Kotaleski, J., & Blackwell, K. T. (2000). The role of protein kinase C in the temporal specificity of purkinje cells. *Soc. Neurosci. Abstr*, 26, 718.